Evaluating the Role of Chromophore Side Group Identity in Mediating Solution-Phase Rotational Motion

Kelly P. Greenough and G. J. Blanchard*

Michigan State University, Department of Chemistry, East Lansing, Michigan 48824-1322

Received: August 22, 2006; In Final Form: November 4, 2006

We report on the rotational diffusion dynamics of the chromophore 7-nitrobenz-2-oxa-1,3-diazole (NBD) in a series of protic and polar aprotic solvents, as a function of the identity of the side group appended to the chromophore amine functionality. The central issue we address is whether or not the side groups play a role in mediating the anisotropic reorientation dynamics of the chromophore. To understand the motional properties of the chromophores in detail, we use both one-photon and two-photon excited fluorescence anisotropy decay measurements, and from these complementary excitation methods, we extract two of the Cartesian components of the rotational diffusion constant, *D*. The experimental data indicate that, regardless of the functionality of the pendant side group, the reorienting moieties exhibit ratios of D_z/D_x in the range 1.8−2.0. There is a small but discernible difference between the substituted chromophores. For all of the substituted NBD chromophores, dielectric friction plays a discernible role in determining their reorientation dynamics.

Introduction

The motion of a molecule in solution is controlled by a number of factors, ranging from its size, shape, and polarity to the nature of its interactions with its immediate environment. It is these interactions that play a critical role in mediating processes such as chemical reaction kinetics, for example. As a result of a broad effort over the past decade or more, a series of chromophores has been identified that are capable of providing information on their local environment with both their time- and frequency-domain responses. Molecules such as pyrene are known to exhibit solvent polarity-dependent fluorescence spectral profiles, and the fluorescence lifetime of this molecule depends sensitively on the amount of oxygen present.[1] Other chromophores have been developed that are tethered to specific structures, allowing them to locate in comparatively well-defined regions of heterogeneous systems. The so-called lock-and-key approach to the examination of crystallization phenomena makes use of chromophores that have as pendant side groups the crystallizing entity.[2−4] This approach to the optical interrogation of molecular-scale phenomena has proven to be useful to a broad range of biological and chemical investigations.

One chromophore that has been used widely for the study of biological and biomimetic systems is 7-nitrobenz-2-oxa-1,3-diazole, NBD.[5−12] The reason for the popularity of this chromophore is that its fluorescence spectral profile and lifetime both depend sensitively on the polarity of its immediate environment. In addition, the chromophore NBD is amenable to synthetic substitution or modification of its amine side group, rendering it useful for localization within heterogeneous systems. A variety of sterols, lipids, and other compounds are available with a pendant NBD chromophore. A recurring question in these studies is the role that the chromophore side group plays in mediating its dynamics. In an effort to address this issue, we have undertaken a study of the reorientation and fluorescence lifetime of NBD possessing several different side groups in a series of polar protic and aprotic solvents. Our data indicate that the reorientation dynamics of the NBD chromophore depend on the identity of the chromophore side group to a limited extent and that we can account for the experimental data in the context of a combination of frictional and dielectric interactions between the dipolar chromophore and its immediate environment.

CHART 1: Structures of the Substituted NBD Chromophores Used in This Work

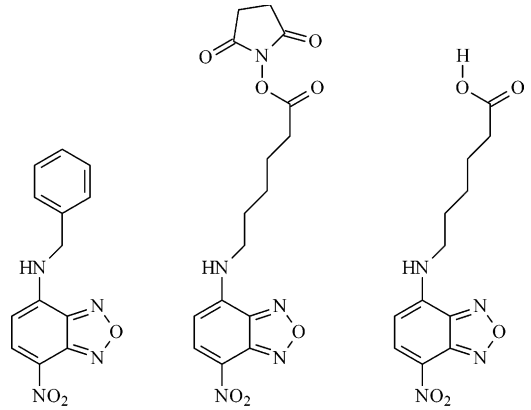

Experimental Section

Materials. The fluorescent probes (Chart 1) succinimidyl 6-(*N*-(7-nitrobenz-2-oxa-1,3-diazol-4-yl)amino) hexanoate (SNBD) and 6-(*N*-(7-nitrobenz-2-oxa-1,3-diazol-4-yl)amino hexanoic acid (NBDHA) were obtained from Molecular Probes, Inc., and used without further purification. The probe 4-benzylamino-7-nitrobenzofurazan (BBD) was purchased from Sigma-Aldrich and was also used as received. The solvents methanol, 1-propanol, 1-butanol, 1-pentanol, dimethyl sulfoxide (DMSO), *N*,*N*-dimethylformamide (DMF), and acetonitrile (ACN) were purchased from Sigma-Aldrich in their highest purity available and

* Author to whom correspondence should be addressed. Email: blanchard@chemistry.msu.edu.

10.1021/jp065423n CCC: $37.00
Published on Web 12/21/2006

were used as received. Ethanol (95%) was distilled in-house. For time-resolved fluorescence measurements, the chromophore concentrations were 10^{-4} M or less in all cases.

Steady-State Measurements. All absorption spectra were recorded on a Cary model 300 double beam UV−visible absorption spectrometer, with 1-nm spectral resolution. All emission spectra were recorded on a Spex Fluorolog 3 spectrometer at a spectral resolution of 3 nm for both excitation and emission monochromators.

Time-Correlated Single-Photon Counting Measurements. All fluorescence lifetime and anisotropy data were collected using a time-correlated single-photon counting (TCSPC) system that has been described in detail elsewhere.[13] We provide a brief recap of its salient properties here. The source laser is a CW mode-locked Nd:YAG laser (Coherent Antares 76-S) that produces 100-ps 1064-nm pulses at 76-MHz repetition rate. The second or third harmonic of the output of this laser is used to excite a cavity dumped dye laser (Coherent 702-2), operating with Rhodamine 610 dye (Exciton, 532-nm pump) for two-photon excitation experiments, or with Stilbene 420 dye (Exciton, 355-nm pump) for one-photon excitation experiments. The dye laser outputs were 5-ps pulses at a repetition rate of 4 MHz for both output wavelengths (460 and 650 nm). Fluorescence transients centered between 535 and 545 nm were detected using a Hamamatsu R3809U microchannel plate photomultiplier tube detector with a Tennelec 454 quad constant fraction discriminator and Tennelec 864 time-to-amplitude converter and biased amplifier used for signal processing. Data were collected using a virtual instrument (VI) written with *LabVIEW 7.1* software. For this system, the instrument response time is typically 35 ps fwhm. Fluorescence transients were collected at polarizations of 0°, 54.7°, and 90° with respect to a vertically polarized excitation pulse.

Results and Discussion

There are several aspects of our experimental data on the chromophores SNBD, BBD, and NBDHA that require discussion. The NBD chromophore is known to exhibit a steady-state spectral response that depends on the polarity of its local environment. We show in Figures 1−3 the absorption and emission spectra of the three chromophores in the solvents used here. We find that the steady-state spectra of the chromophores change very little with the identity of the alcohol solvent (Figures 1a−3a), but there is a marked variation in absorption and emission maxima in the polar aprotic solvents ACN, DMF, and DMSO (Figures 1b−3b). For a given chromophore, the spectra in ACN are most similar to those in the alcohols, and greater red-shifting of both absorption and emission bands is seen for DMF and DMSO. Attempting to understand these spectral shifts in the context of solvent properties or polarity indices does not yield any insight into the chemical basis for these spectral shifts. Likewise, it appears that the Stokes shifts for these molecules do not change significantly or in a manner correlated to any solvent property or polarity index that we have tested. These spectra provide us with the information needed to perform the time-resolved experiments but give limited insight into the chemical and/or physical basis for the observed band positions and Stokes shifts. For this reason, we have examined the emission bands of these chromophores in the time domain.

We consider next the relationship between the chromophore fluorescence lifetime and the polarity of the medium in which the chromophore resides. We note that the fluorescence lifetimes of BBD, SNBD, and NBDHA are quite similar, and this is not surprising. The NBD chromophore is known to exhibit a solvent

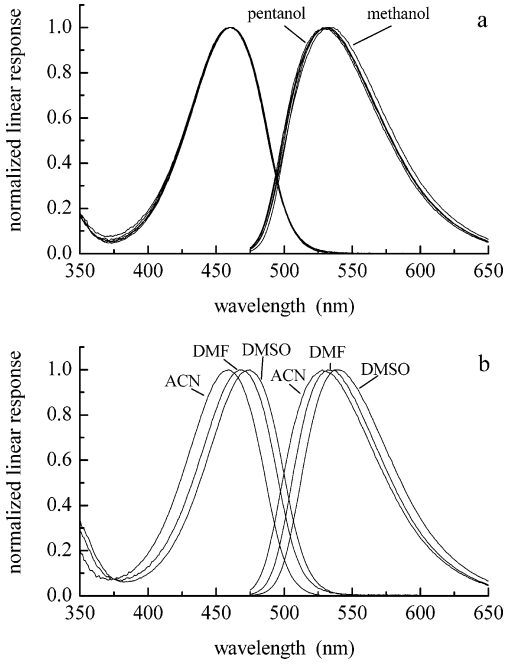

Figure 1. (a) Normalized absorption and emission spectra of BBD in the n-alcohols methanol through 1-pentanol. (b) Normalized absorption and emission spectra of BBD in the polar aprotic solvents acetonitrile (ACN), *N*,*N*-dimethyl formamide (DMF), and dimethyl sulfoxide (DMSO).

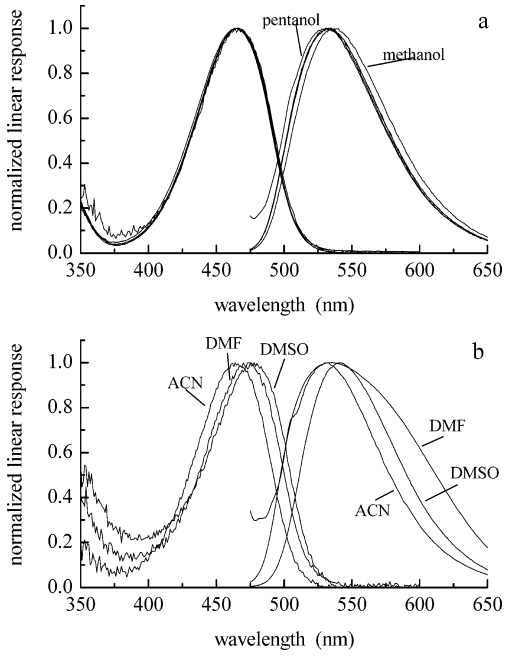

Figure 2. (a) Normalized absorption and emission spectra of SNBD in the n-alcohols methanol through 1-pentanol. (b) Normalized absorption and emission spectra of SNBD in the polar aprotic solvents acetonitrile (ACN), *N*,*N*-dimethyl formamide (DMF), and dimethyl sulfoxide (DMSO).

polarity-dependent fluorescence lifetime,[5−7,9−11] but the issue of what comprises "solvent polarity" is not well-understood. We have examined whether or not there is a correlation between the fluorescence lifetime of the NBD chromophore and a variety of solvent properties such as dielectric constant, refractive index, Debye dielectric relaxation time, and solvent viscosity. We have found no correlation between fluorescence lifetime and any of these solvent properties, which is not surprising. The nanosecond time scale over which the chromophore population decays

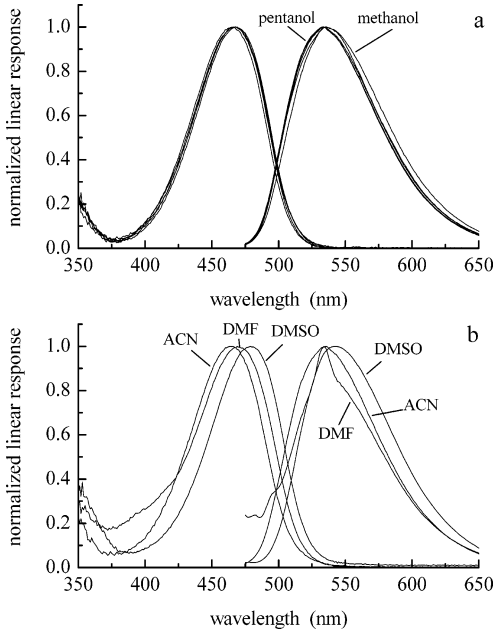

Figure 3. (a) Normalized absorption and emission spectra of NBDHA in the n-alcohols methanol through 1-pentanol. (b) Normalized absorption and emission spectra of NBDHA in the polar aprotic solvents acetonitrile (ACN), *N*,*N*-dimethyl formamide (DMF), and dimethyl sulfoxide (DMSO).

following excitation differs from the characteristic time scales which the above parameters sense, in many cases by several orders of magnitude. The interactions between solvent and solute must derive from dipole−dipole and dipole−induced dipole coupling, but the typical measures of solvent−solvent coupling listed above do not access the region(s) of the frequency-dependent dielectric response of the medium that dominate solvent−solute interactions.[14,15]

The literature is replete with attempts to create solvent polarity scales, with the most notable being the *py* scale,[16,17] the π^* scale,[18−21] and the $E_T(30)$ scale.[22,23] The *py* scale is based on the emission spectrum of pyrene, which is sensitive to solvent mediation of the vibronic coupling between its S_1 and S_2 electronic states.[1] For the π^* and $E_T(30)$ scales, the solvent "polarity" is gauged by the spectral shifts of a polar dye molecule, with the mechanism(s) of these spectral shifts not being well-understood at the molecular level. Perhaps because of this lack of fundamental understanding, these latter two solvent polarity scales have been related to various solvent properties through phenomenological linear free energy relationships, with each factor weighted according to the creator(s) of the polarity scale. It is useful to note that, despite the success of these polarity scales, the system properties that are empirically factored into them are, for the most part, related to the polarizability of the solvent in some manner. These polarity scales can, in fact, prove useful, as is the case here. We find that the fluorescence lifetime of the NBD chromophore correlates reasonably well with the $E_T(30)$ polarity scale (Figure 4, Table 1). This information is useful for predictive or comparative purposes of estimating the polarity of the chromophore local environment. Because NBD derivatives find wide use in the investigation of biological systems such as lipid bilayer structures, the correlation we report in Figure 4 is of potential utility in understanding the average chemical environments of complex biological systems. Unfortunately, the analogous correlation does not exist in the frequency domain, between the steady-state spectral maxima and the $E_T(30)$ scale. This is not surprising given the extent to which inhomogeneous

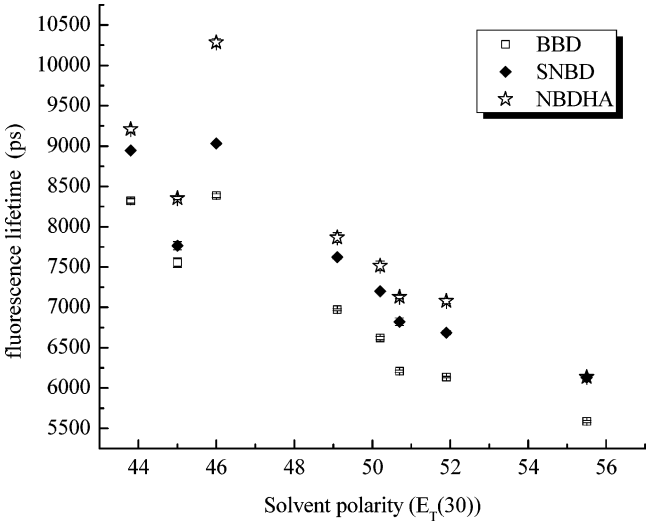

Figure 4. Dependence of chromophore fluorescence lifetime on solvent polarity. The solvent polarity is given in the form of the $E_T(30)$ scale, and the fluorescence lifetimes are in picoseconds. □ = BBD, ♦ = SNBD, and ☆ = NBDHA.

TABLE 1: Fluorescence Lifetimes of the Chromophores BBD, SNBD, and NBDHA in the Solvents Used in This Work[a]

solvent	$E_T(30)$ polarity	BBD τ_{fl} (ps)	SNBD τ_{fl} (ps)	NBDHA τ_{fl} (ps)
ACN	46.0	8385 ± 22	9031 ± 5	10283 ± 51
MeOH	55.5	5585 ± 13	6129 ± 14	6136 ± 21
DMF	43.8	8319 ± 27	8944 ± 16	9208 ± 35
EtOH	51.9	6136 ± 10	6685 ± 24	7078 ± 32
PrOH	50.7	6208 ± 16	6822 ± 46	7129 ± 22
DMSO	45.0	7553 ± 60	7764 ± 52	8354 ± 19
BuOH	50.2	6620 ± 20	7199 ± 17	7515 ± 59
PeOH	49.1	6972 ± 12	7622 ± 23	7866 ± 60

[a] Solvent polarities according to the $E_T(30)$ scale were taken from ref 22. Uncertainties reported here are $\pm 1\sigma$ for at least six individual determinations. Lifetimes were the same for both one- and two-photon excitation to within the uncertainty of the measurement.

broadening contributes to the spectral features of this complex organic chromophore.

We note that, as the solvent polarity increases, the lifetime of the chromophore(s) decreases. This is expected because of the polar nature of the chromophore. Despite the poorly defined term of solvent polarity, we expect qualitatively that, as the strength of (polar) interactions increases between solvent and solute, the greater opportunity there is for structural and/or electronic wavefunction distortion of the solute. Such interactions between solvent and solute serve to increase the opportunity for nonradiative decay from the solute excited state.

We consider next the rotational diffusion properties of these chromophores. Because the theoretical foundation of reorientation measurements is well-established, there is a wealth of information available from this type of measurement. We use both one-photon and two-photon excitation, because they provide complementary information. For both modes of excitation, we monitor emission from the same excited state. We recap the information available from the two excitation methods and what we can extract from the experimental data for BBD, SNBD, and NBDHA.

One-Photon Excited Fluorescence Anisotropy. In one-photon excited anisotropy measurements, the sample is excited by a vertically polarized light pulse, and the resulting emission

is collected parallel and perpendicular to the incident beam. The induced orientational anisotropy is given by

$$R(t) = \frac{I_{||}(t) - I_{\perp}(t)}{I_{||}(t) + 2I_{\perp}(t)} \quad (1)$$

where $I_{||}(t)$ is the intensity of emission collected at a polarization angle of 0° with respect to the incident vertical polarization, and $I_{\perp}(t)$ is the intensity of emission collected at a polarization angle of 90° with respect to the incident polarization. Chemically useful information is contained in the decay time constant(s) of $R(t)$ (eq 1). $R(t)$ can contain up to five exponential decays in theory, but only one or two decays are observed experimentally. The values of $R(0)$ can range from −0.2 to 0.4 for one-photon excited anisotropy measurements, depending on the angle between the excited and emitting transition dipole moments.

The relationship between the anisotropy decay obtained experimentally and the molecular properties of the rotating molecule have been described by Chuang and Eisenthal.[24] These molecular properties include the rotational diffusion constants and the angle between the excited and emitting transition dipole moments. The typical assignment of Cartesian axes to the chromophore are to have the *z*-axis perpendicular to the molecular π-system plane and the transition dipole lying either along the *x* (long) axis or the *y* (short) axis of the molecular plane. We follow this convention for the NBD chromophores considered here. Two limiting cases can be examined to evaluate the functionality of the anisotropy decay. By estimating the shape of the volume swept out by the rotating molecule as oblate ($D_z \neq D_x = D_y$) or prolate ($D_x \neq D_y = D_z$) rotors, we can simplify Chuang and Eisenthal's equations significantly. Even with these simplifications, there remains ambiguity in determining whether the prolate or oblate rotor shape best represents the molecule in question because of the orientation of the transition dipoles relative to the rotor axes. For parallel absorbing and emitting transition dipole moments, oriented along the long (*x*) axis of the ellipsoid of rotation, the functional forms of $R(t)$ are[24]

$$\text{oblate} \quad R(t) = 0.1\exp[-(2D_x + 4D_z)t] + 0.3\exp(-6D_x t) \quad (2)$$

$$\text{prolate} \quad R(t) = 0.4\exp(-6D_z t) \quad (3)$$

Similarly, for parallel absorbing and emitting transitions that are short (*y*) axis polarized

$$\text{oblate} \quad R(t) = 0.4\exp[-(4D_x + 2D_z)t] \quad (4)$$

$$\text{prolate} \quad R(t) = 0.1\exp[-(4D_x + 2D_z)t] + 0.3\exp(-6D_z t) \quad (5)$$

For the NBD derivatives we have examined, all anisotropy decays are single exponential (an example is provided in Figure 5), a condition consistent with either a prolate rotor with a long-axis polarized transition or an oblate rotor with a short-axis polarized transition. Because of this ambiguity, we have also used two-photon excitation to provide complementary information and thus resolve the Cartesian components of the rotational diffusion constant.

Two-Photon Excited Fluorescence Anisotropy. Two-photon excitation involves the photoselection of an anisotropic orientational distribution via the two-photon tensor, *S*, in contrast to the transition dipole moment, μ, accessed by one-photon excitation. Which two-photon tensor elements are accessed depends on the polarization of the incident light. Induced

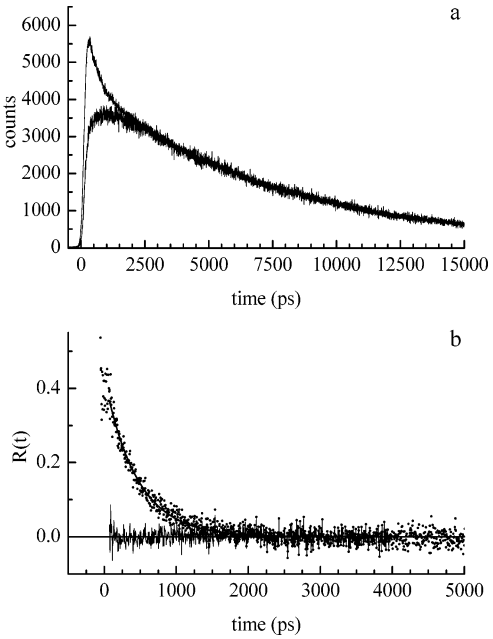

Figure 5. (a) Representative $I_{||}(t)$ and $I_{\perp}(t)$ data for SNBD in 1-pentanol with one-photon excitation. (b) Corresponding $R(t)$ function generated from the data according to eq 1. The line through the data is the best fit single-exponential decay function, with the residuals of the fit being distributed around zero intensity.

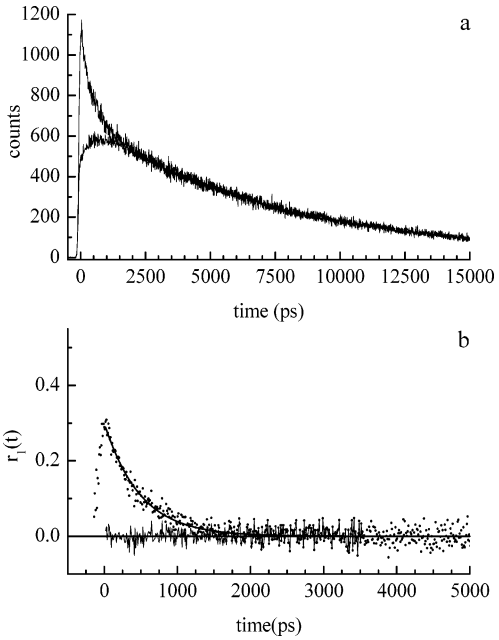

Figure 6. (a) Representative $I_{||}(t)$ and $I_{\perp}(t)$ data for SNBD in 1-pentanol with linearly polarized two-photon excitation. (b) Corresponding $R(t)$ function generated from the data according to eq 6. The line through the data is the best fit single-exponential decay function, with the residuals of the fit being distributed around zero intensity.

orientational anisotropy decay functions are generated for both linearly ($r_1(t)$) and circularly ($r_2(t)$) polarized excitation and are given by

$$r_1(t) = \frac{I_{||}^{\text{linear}}(t) - I_{\perp}^{\text{linear}}(t)}{I_{||}^{\text{linear}}(t) + 2I_{\perp}^{\text{linear}}(t)}$$

$$r_2(t) = \frac{I_{||}^{\text{circular}}(t) - I_{\perp}^{\text{circular}}(t)}{2I_{||}^{\text{circular}}(t) + I_{\perp}^{\text{circular}}(t)} \quad (6)$$

For both excitation polarizations, the anisotropy decays are characterized by two time constants, τ_0 and τ_2, weighted according to the spectroscopic and dynamical properties of the chromophore.[25−27] The anisotropy decay for either two-photon

$$r_1(t) = r_1(0)[c_0 \exp(-t/\tau_0) + c_2 \exp(-t/\tau_2)]$$
$$r_2(t) = r_2(0)[d_0 \exp(-t/\tau_0) + d_2 \exp(-t/\tau_2)] \quad (7)$$

excitation polarization should contain two exponentials, but this is not seen in all cases. Our data are characterized by a single-exponential decay time constant, and there are two possible explanations for this finding. The first is that the two time constants τ_0 and τ_2 are similar enough that they cannot be resolved outside of the experimental uncertainty. The other possibility is that some of the prefactors in eqs 7 are too small to observe. The prefactors c_i and d_i have been described in detail elsewhere,[8,25−27] and we present them for illustrative purposes.

$$c_0 = \frac{(\sqrt{3}a + b)[3(\sqrt{3}a + b)S_{xx}^2 + 3(-\sqrt{3}a + b)S_{yy}^2 + 2bS_{xx}S_{yy} + 4bS_{xy}^2]}{7N^2(3S_{xx}^2 + 3S_{yy}^2 + 2S_{xx}S_{yy} + 4S_{xy}^2)} \quad (8)$$

$$c_2 = \frac{(a - \sqrt{3}b)[3(a - \sqrt{3}b)S_{xx}^2 + 3(a + \sqrt{3}b)S_{yy}^2 + 2aS_{xx}S_{yy} + 4aS_{xy}^2]}{7N^2(3S_{xx}^2 + 3S_{yy}^2 + 2S_{xx}S_{yy} + 4S_{xy}^2)} \quad (9)$$

$$d_0 = \frac{(\sqrt{3}a + b)[(\sqrt{3}a + b)S_{xx}^2 + (-\sqrt{3}a + b)S_{yy}^2 - 4bS_{xx}S_{yy} + 6bS_{xy}^2]}{14N^2(S_{xx}^2 + S_{yy}^2 - S_{xx}S_{yy} + 3S_{xy}^2)} \quad (10)$$

$$d_2 = \frac{(a - \sqrt{3}b)[(a - \sqrt{3}b)S_{xx}^2 + (a + \sqrt{3}b)S_{yy}^2 - 4aS_{xx}S_{yy} + 6aS_{xy}^2]}{14N^2(S_{xx}^2 + S_{yy}^2 - S_{xx}S_{yy} + 3S_{xy}^2)} \quad (11)$$

$$a = \sqrt{3}(D_y - D_x)$$

$$b = 2D_z - D_y - D_x + 2\Delta$$

$$N^2 = a^2 + b^2$$

$$\Delta = (D_x^2 + D_y^2 + D_z^2 - D_xD_y - D_yD_z - D_xD_z)^{1/2} \quad (12)$$

In order to obtain more information about the rotational diffusion coefficients, we return to the limiting cases of prolate ($D_x \neq D_y = D_z$) and oblate ($D_z \neq D_x = D_y$) rotors. Using these ellipsoidal shapes to simplify eqs 12, we obtain the prefactors in eqs 8−11 for the terms c and d as follows:

Prolate: $\sqrt{3}a + b = 2\sqrt{3}(D_z - D_x) \quad a - \sqrt{3}b = 0$

Oblate: $\sqrt{3}a + b = 4(D_z - D_x)$
$a - \sqrt{3}b = 4\sqrt{3}(D_x - D_z)$

Given the fact that we obtain a single exponential anisotropy decay for both one-photon (Figure 5) and two-photon (Figures 6 and 7) excitation in these experiments, the experimental data are most consistent with the NBD chromophores reorienting as prolate rotors in the systems we have examined. For a prolate rotor, the time constant τ_0 for two-photon excitation is

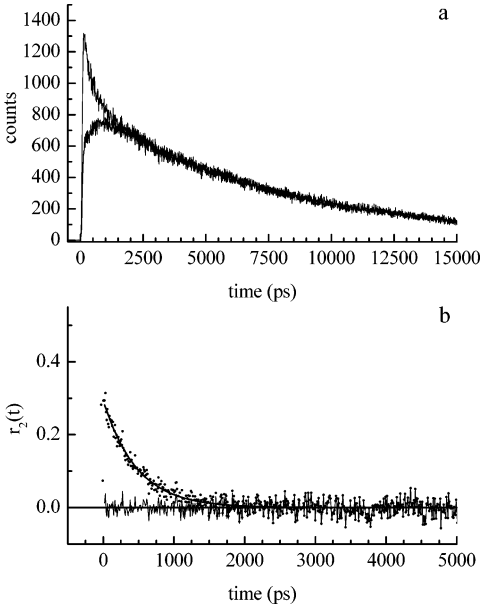

Figure 7. (a) Representative $I_{\parallel}(t)$ and $I_{\perp}(t)$ data for SNBD in 1-pentanol with circularly polarized two-photon excitation. (b) Corresponding $R(t)$ function generated from the data according to eq 6. The line through the data is the best fit single-exponential decay function, with the residuals of the fit being distributed around zero intensity.

$$\tau_0 = \frac{S_{xx}^2(7D_x + 17D_z) - 4S_{yy}^2(2D_x - D_z) + (S_{xx}S_{yy} + 2S_{xy}^2)\left[\frac{3(D_z^2 + 2D_zD_x)}{2D_x + D_z} + 4D_x - D_z\right]}{8(D_z^2 + 2D_xD_z)(6S_{xx}^2 - 3S_{yy}^2 + S_{xx}S_{yy} + 2S_{xy}^2)} \quad (13)$$

By setting $S_{yy} = 1$ and extracting normalized values of S_{xx} and S_{xy} from $r_1(0)$ and $r_2(0)$, then using the value of D_z obtained from the one-photon measurements (eq 3), we can extract D_x from the two-photon excitation data.

We present in Tables 2−4 the experimental reorientation times and the resulting values of D_z and D_x that we extract from our anisotropy data as a function of chromophore and solvent. As expected, the reorientation times for one-photon excitation and two-photon excitation of each chromophore differ, in some cases quite noticeably. This is an expected result, as is clear from comparing eq 3 with eq 13, for example. These data show that, while there are subtle differences between the substituted chromophores, they all produce qualitatively the same result of $D_z/D_x \approx 2$. This finding is significant in that it implies that the side groups exert a limited influence on the motional properties of these molecules, which is likely the result of averaging motions over a large number of side group conformations for all three chromophores.

We note that the assignment of a prolate effective rotor shape for these chromophores is based on the observation of single-exponential decays for both the one- and two-photon excitation data. It is, of course, possible that there could be two exponential decays present in our data that remain unresolved due either to the similarity of the time constants or to the limited S/N ratio of the experimental data. In the limit that the time constants are too similar to resolve, the physical picture that emerges from a prolate rotor would change little, and the conclusions drawn from interpreting the data as single exponentials would not change. If the latter were the case, we would expect to see at least hints of deviation from single exponential behavior in the

TABLE 2: Experimental Reorientation Times for BBD Using One-Photon Excitation (1) and Two-Photon Excitation with Linear Polarization (2L) and Circular Polarization (2C)[a]

solvent	viscosity η, (cP)	$\tau_{OR}(1)$ (ps)	$\tau_{OR}(2L)$ (ps)	$\tau_{OR}(2C)$ (ps)	D_z (MHz)	D_x (MHz)	D_z/D_x
ACN	0.37	88 ± 9	72 ± 15	92 ± 9	1894	959	2.0
MeOH	0.54	96 ± 13	79 ± 11	79 ± 6	1736	900	1.9
DMF	0.79	102 ± 3	103 ± 6	123 ± 14	1634	846	1.9
EtOH	1.07	139 ± 10	148 ± 15	140 ± 6	1199	595	2.0
PrOH	1.95	199 ± 10	205 ± 7	199 ± 11	838	419	2.0
DMSO	1.99	170 ± 27	151 ± 4	196 ± 23	980	428	2.3
BuOH	2.54	267 ± 25	249 ± 19	252 ± 7	624	304	2.1
PeOH	3.61	333 ± 19	365 ± 32	346 ± 24	501	247	2.0

[a] Values of D_x and D_z are extracted from the experimental data according to eqs 3 and 13. Uncertainties reported here are $\pm 1\sigma$ for at least six individual determinations.

TABLE 3: Experimental Reorientation Times for SNBD Using One-Photon Excitation (1) and Two-Photon Excitation with Linear Polarization (2L) and Circular Polarization (2C)[a]

solvent	viscosity η, (cP)	$\tau_{OR}(1)$ (ps)	$\tau_{OR}(2L)$ (ps)	$\tau_{OR}(2C)$ (ps)	D_z (MHz)	D_x (MHz)	D_z/D_x
ACN	0.37	125 ± 3	81 ± 22	76 ± 2	1333	826	1.6
MeOH	0.54	182 ± 15	113 ± 6	112 ± 2	916	497	1.8
DMF	0.79	177 ± 5	140 ± 7	136 ± 11	942	535	1.8
EtOH	1.07	238 ± 25	179 ± 2	195 ± 118	700	396	1.8
PrOH	1.95	351 ± 31	292 ± 14	328 ± 7	474	269	1.8
DMSO	1.99	285 ± 15	239 ± 18	288 ± 18	585	322	1.8
BuOH	2.54	398 ± 18	324 ± 19	396 ± 5	419	246	1.7
PeOH	3.61	477 ± 19	465 ± 14	499 ± 19	349	187	1.9

[a] Values of D_x and D_z are extracted from the experimental data according to eqs 3 and 13. Uncertainties reported here are $\pm 1\sigma$ for at least six individual determinations.

TABLE 4: Experimental Reorientation Times for NBDHA Using One-Photon Excitation (1) and Two-Photon Excitation with Linear Polarization (2L) and Circular Polarization (2C)[a]

solvent	viscosity η, (cP)	$\tau_{OR}(1)$ (ps)	$\tau_{OR}(2L)$ (ps)	$\tau_{OR}(2C)$ (ps)	D_z (MHz)	D_x (MHz)	D_z/D_x
ACN	0.37	50 ± 3	52 ± 3	49 ± 3	3370	1887	1.8
MeOH	0.54	131 ± 24	112 ± 10	111 ± 10	1270	610	2.1
DMF	0.79	162 ± 11	134 ± 13	109 ± 3	1030	599	1.7
EtOH	1.07	174 ± 6	158 ± 13	180 ± 21	960	566	1.7
PrOH	1.95	302 ± 13	283 ± 12	339 ± 50	550	324	1.7
DMSO	1.99	273 ± 10	204 ± 22	250 ± 16	610	352	1.7
BuOH	2.54	570 ± 26	402 ± 20	426 ± 56	290	165	1.8
PeOH	3.61	724 ± 15	456 ± 4	539 ± 35	230	128	1.8

[a] Values of D_x and D_z are extracted from the experimental data according to eqs 3 and 13. Uncertainties reported here are $\pm 1\sigma$ for at least six individual determinations.

residuals of the fits to the data. In no cases do we observe any such indication. While the interpretation of our data is ultimately limited by the *S*/*N* ratio of the data, as is the case for many experimental studies, the consistency and reproducibility of our findings lend confidence to our interpretation of single exponential anisotropy decays.

We consider next how to relate our findings to solvent−solute interactions. The relationship between molecular rotational motion and the properties of the surrounding solvent medium has been described by the modified Debye−Stokes−Einstein model[28]

$$\tau_{DSE} = \frac{\eta V f}{k_B T S} \tag{14}$$

where the time constant for rotational motion, τ_{DSE}, is determined from the anisotropy decay data. The term η is the solvent bulk viscosity, V is the hydrodynamic volume[29] of the rotating moiety, f is a frictional interaction term, taken to be 1 for polar systems, and S is the shape factor derived by Perrin[30] to account for nonspherical solutes. The quantity τ_{DSE} is equal to $6D^{-1}$, where $D = {}^1/_3(D_x + D_y + D_z)$. We can thus relate the predictions of the DSE model to the experimental data.

We show in Tables 2−4 the experimentally measured one-photon excited reorientation times and compare these data to the predictions of the DSE model with $S = 0.667$, calculated for a prolate rotor with an aspect ratio of 2[31,32] (Table 5). In all cases, the experimental reorientation times are longer than those predicted by eq 14 (Figure 8, dashed line vs experimental data). Such a relationship between experiment and model has been seen for a number of molecules,[33−35] and the origin(s) of such a discrepancy have been ascribed to a number of factors. Certainly, some portion of this difference arises from the DSE model itself. Equation 14 was derived for an ellipsoidal solute reorienting in a continuum solvent, thereby accounting only for frictional interactions. To compound matters, the estimation of V and S can give rise to significant uncertainty because of the intrinsic dynamics and variability in the range of structural conformations that these chromophores can take on over time. Also, depending on the solvent system used, strong and persistent solvent−solute interactions can give rise to a rotating entity that is larger, on average, than the bare chromophore.[4,34,35] Such a solvent-attachment approach to understanding experimental reorientation data has been useful for solvents capable of hydrogen bonding.[36] For solvents that are not capable of

TABLE 5: Calculated Dielectric Friction Time Constants, DSE Reorientation Time Constants and Their Sum, Reported at τ_{OR}[a]

				BBD			SNBD			NBDHA		
solvent	viscosity η, (cP)	dielectric constant, ϵ_0	τ_D (ps)	τ_{df} (ps)	τ_{DSE} (ps)	τ_{OR} (ps)	τ_{df} (ps)	τ_{DSE} (ps)	τ_{OR} (ps)	τ_{df} (ps)	τ_{DSE} (ps)	τ_{OR} (ps)
ACN	0.37	38.0	4	0.2	30	30	0.2	40	40	0.2	33	33
MeOH	0.54	33.7	56	3.4	42	45	3.4	58	61	2.5	48	51
DMF	0.79	36.7	12	0.8	61	62	0.8	85	86	0.6	70	71
EtOH	1.07	24.5	337	30.6	82	113	29.3	115	144	24	94	118
PrOH	1.95	20.5	430	46.5	151	198	44.4	210	254	36	174	210
DMSO	1.99	46.5	21	0.8	153	154	0.8	214	215	0.6	177	178
BuOH	2.54	17.5	668	75.4	198	273	72.1	271	343	58	225	283
PeOH	3.61	13.9	927	129	280	409	123	388	511	99	321	420

[a] Solvent properties viscosity, dielectric constant, and Debye dielectric relaxation time constant are from refs 34, 47, 53. For the calculation of τ_{DSE} ($S = 0.667$) (eq 14), $V = 215$ Å^3 for BBD; $V = 297$ Å^3 for SNBD; $V = 245$ Å^3 for NBDHA.[29] For the calculation of τ_{df}, $a = 3.7$ Å and $\mu^* = 10.6$ D for BBD; $a = 4.1$ Å and $\mu^* = 12.2$ D for SNBD; $a = 3.9$ Å and $\mu^* = 9.9$ D for NBDHA.

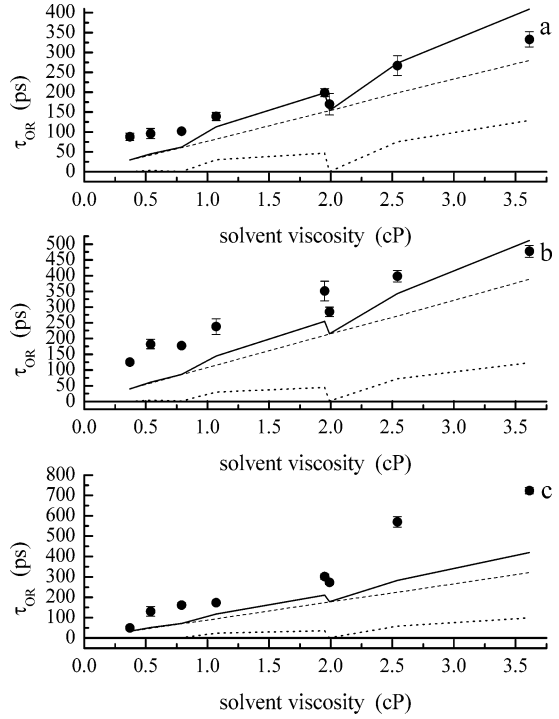

Figure 8. (a) One-photon experimental reorientation times (●) for BBD as a function of solvent viscosity. The dashed line is calculated from the DSE model (eq 14), the dotted line is the calculated dielectric friction contribution (eq 15), and the solid line is the sum of the two model contributions. (b) One-photon experimental reorientation times (●) for SNBD as a function of solvent viscosity, with the dashed, dotted, and solid lines having the same assignments as for panel (a). (c) One-photon experimental reorientation times (●) for NBDHA as a function of solvent viscosity, with the dashed, dotted, and solid lines having the same assignments as for panel (a).

forming H-bonds, such an explanation is not appropriate. Another approach to understanding such data has been to postulate that the reorienting molecule, in certain circumstances, can possess added effective volume owing to the conformation of its side groups. As noted above, such an explanation is difficult to support because of the labile nature of the side groups that would have to be responsible for creating any such "volume" and the fact that, within the most widely accepted model for the calculation of hydrodynamic volume, there is no means to account for conformational variations within a given molecule.[29] A third explanation for the difference between experiment and theory is that the frictional interactions between the solvent and the solute are very strong, giving rise to values of f that exceed unity. Such interactions have been examined theoretically,[37] but values of f in excess of unity derived from experimental data are necessarily suspect. Assigning physical or chemical significance to such an explanation would hinge on the identification of strong, persistent solvent−solute interactions such as hydrogen bonding or dipole−dipole interactions.

In addition to the reasons put forth above, there can be other contributions to the interactions between solvent and solute. The dielectric coupling between the solvent medium and the solute can also contribute to the solute reorientation times. Dielectric friction is a mechanism for solvent−solute interactions that has a well-established theoretical foundation,[38−46] and it has proven useful in explaining a host of reorientation data for sometimes complex systems.[47] In this model, there are two contributions to solvent−solute interactions: viscoelastic frictional forces, which are accounted for through the DSE model (eq 14), and dielectric interactions, which can be modeled by

$$\tau_{df} = \frac{\mu^{*2}(\epsilon - 1)\tau_D}{k_B T a^3 (2\epsilon + 1)^2} \tag{15}$$

where μ^* is the solute excited-state dipole moment, ϵ is the zero-frequency dielectric constant of the solvent medium, τ_D is the Debye relaxation time of the solvent, and a is the radius of the sphere approximating the solute cavity in the solvent. In this model, the contribution of dielectric friction to the overall reorientation time of the chromophore depends on the solute property μ^{*2}/a^3, which effectively represents the torque exerted on the solvent by the solute as it moves, the solvent susceptibility to this force, and the characteristic time constant for solvent motions, τ_D. It is this latter term that plays a dominant role in determining the contribution from dielectric friction. For hydrogen-bonding solvents, τ_D is relatively long, reflecting the extensive H-bonding network formed in alcohols, and in aprotic solvents, τ_D is short, mediated primarily by dipole−dipole or dispersion interactions. This dependence on τ_D provides an important signature that can be compared to experimental data, as we consider below.

A word is in order about the values of μ^* we used in the calculation of τ_{df}. We have calculated the excited-state dipole moments for BBD, SNBD, and NBDHA at the semiempirical level, using *Hyperchem v. 6.0* with the PM3 parametrization. While it would be preferable to obtain an experimental estimate of the dipole moments of these molecules, none of them exhibit a sufficient solvatochromaticity, nor are there any reliable experimental data available on the ground-state dipole moments of these molecules. Thus, we are left to estimate the values of μ^*, and experience has indicated that the PM3 parametrization provides useful results for polar organic chromophores such as NBD.

We show in Table 5 and Figure 8 the comparison of our experimental data to model predictions where τ_{OR} (solid line) is the sum of τ_{DSE} (eq 14, dashed line) and τ_{df} (eq 15, dotted line). There are a number of interesting features to be noted in the comparison of the experimental data to the model. First, we note that in all cases the experimental reorientation time is longer than that calculated by the model. As discussed above, this systematic difference between model and data can be accounted for either in the context of an underestimation of the frictional terms, a systematic error in the calculation of the hydrodynamic volume, *V*, or direct solvent−solute interactions. We note that the data for NBDHA, the only solute studied here that has a side group capable of participating strongly in H-bonding interactions, provides the greatest difference between model and experiment. It is likely that strong solvent−solute interactions, in some cases approaching "solvent attachment", are responsible for at least a portion of this difference. We also consider that, for BBD and SNBD, the experimental reorientation times do not regress to a prediction of $\tau_{OR} \approx 0$ for zero viscosity. Such behavior has been seen before, and it has sometimes been explained in the context of the inertial contributions of molecular motion in the limit of zero viscosity. When inertial contributions are calculated for dyes similar in size to these NBD derivatives, the inertial contributions account for only a few picoseconds at most.[48] Another possible explanation is that for low solvent viscosities there is a different boundary condition for frictional solvent−solute interactions than there is for higher-viscosity systems. We work with several solvents of relatively low viscosity (ACN, MeOH, DMF), and if such a change in boundary condition were to occur with increasing viscosity, it is likely that we would sense it. The origin of the nonzero intercept for the data in Figure 8 will require further investigation to understand in detail.

For all of the chromophores we have examined here, there is a significant feature in the experimental data. The data for 1-propanol ($\eta = 1.95$ cP) and DMSO ($\eta = 1.99$ cP) are consistent in that for all chromophores the reorientation time of DMSO is always faster than that of 1-propanol (Figure 8). This finding stands in contrast to the DSE model (eq 14) but is predicted accurately in the context of dielectric friction contributions to the data (eq 15). The apparent anomaly results from the short τ_D of DMSO compared to that for 1-propanol, and this feature is modeled well by eq 15. This feature is not seen as prominently for the other polar aprotic solvents that are characterized by short τ_D values, because the τ_D values for the alcohols in the same viscosity range are also short. There is insufficient contrast between methanol and acetonitrile to resolve contributions from dielectric friction, but there is a small observable effect for DMF and a prominent effect seen for comparing DMSO to 1-propanol data (Figure 8). We take the comparison of the functional form of the data and the model to indicate that dielectric friction does, in fact, contribute to our results.

The offset between experiment and model cannot be explained fully in the context of the DSE model. It is also possible that the contribution from dielectric friction has not been estimated correctly owing to the limitations of the model. The systematic difference between model and experiment could result from our use of the calculated solute excited-state dipole moments or from the limitations associated with the assumption of the spherical solute shape, as implied by the a^3 term. In Table 5, where the frictional and dielectric contributions to the overall model reorientation time are indicated, it is clear that dielectric friction plays a more important role in alcohols than it does in aprotic solvents, underscoring the importance of persistent solvent organization as expressed through τ_D. While we have found literature values for τ_D, we recognize that this is a difficult quantity to obtain and that there may be significant uncertainties in the values we use. We note that for both the frictional and dielectric contributions to the model, when there is a systematic difference between model and experiment, the implication is that one of the quantities used in the calculations is consistently underestimated. It is also possible that there are other contributions to the experimental data that remain unaccounted for, such as changes in the frictional boundary condition between solvent and solute, as the ratio of solvent to solute size varies systematically. If there is any indication of such an effect, it appears to be most prominent for BBD (Figure 8a) and SNBD (Figure 8b), where the smallest solvents appear to be modeled least well. Such a finding would appear to stand in conflict with the DSE model, which was derived under the assumption of a continuum solute, a condition approximated most closely by small solvents and large solutes. Regardless of these subtle features in the data, there is overall good agreement between model and experiment, as shown in Figure 8.

We recognize that invoking dielectric friction as a contributor to our experimental data is difficult to verify by other means, especially in light of other systems that have shown varying contributions from this same effect. Several studies have concluded that dielectric friction does not contribute significantly to their data, even with polar solvents and solutes.[49,50] In those cases, coumarin derivatives were used as the solutes and the interpretation of the data may have been complicated by the presence of multiple excited electronic states in close energetic proximity.[51] In other cases, where systems where comparatively less polar chromophores such as DPP and DMDPP have been used, dielectric friction can contribute to the motional behavior of these molecules.[52] It would appear that the contribution of dielectric friction to experimental reorientation data can be important, but the extent to which dielectric friction contributes is system-dependent. The fact that the functional form of our experimental data match relatively well with the predictions of eq 15 suggest that NBD derivatives do in fact experience dielectric friction in polar solvents.

Conclusions

We have shown in this work that, despite the different side groups present on the NBD chromophores, the dynamics of the molecules are fundamentally quite similar. In all cases, the fluorescence lifetime of the NBD chromophore exhibits the same solvent polarity dependence, indicating that the side groups are neither coupled strongly to the electronic excited state of the NBD chromophore, nor is there a significant steric interaction between side group and chromophore that interferes with chromophore−solvent interactions.

The rotational diffusion data for both one- and two-photon excitation of the NBD chromophore reveal remarkably similar motional behavior for the three molecules, analogous to the lifetime data. The use of both one- and two-photon excitation provides complementary information and allows the evaluation of the ratio of the Cartesian components of the rotational diffusion constant. For the three molecules we have studied, $D_z/D_x \approx 2$. When our experimental reorientation data are compared to the well-established Debye−Stokes−Einstein model, we find that in all cases the experimental reorientation time is substantially longer than predicted. We account for this discrepancy to a substantial extent by considering the role that dielectric friction plays. When dielectric friction is accounted

for, the reorientation times predicted by the model are much more similar to the experimental data, including the apparent discrepancy between H-bonding alcohol solvents and polar aprotic solvents. Taken collectively, our measurements show that the identity of the side group on the NBD chromophore plays little measurable role in determining the dynamics of the NBD chromophore, and both frictional and dielectric effects must be taken into account to understand the comparatively strong interactions between NBD and polar solvents.

Acknowledgment. We are grateful to the National Science Foundation for support of this work through grant 0445492.

References and Notes

(1) Karpovich, D. S.; Blanchard, G. J. *J. Phys. Chem.* **1995**, *99*, 3951.
(2) Rasimas, J. P.; Berglund, K. A.; Blanchard, G. J. *J. Phys. Chem.* **1996**, *100*, 17034.
(3) Rasimas, J. P.; Berglund, K. A.; Blanchard, G. J. *J. Phys. Chem.* **1996**, *100*, 7220.
(4) Rasimas, J. P.; Blanchard, G. J. *J. Phys. Chem.* **1995**, *99*, 11333.
(5) Chapman, C. F.; Liu, Y.; Sonek, G. J.; Tromberg, B. J. *Photochem. Photobiol.* **1995**, *62*, 416.
(6) Chattopadhyay, A.; London, E. *Biochim. Biophys. Acta*, Biomembranes **1988**, *938*, 24.
(7) Fery-Forgues, S.; Fayet, J.-P.; Lopez, A. *J. Photochem. Photobiol., A* **1993**, *70*, 229.
(8) Greenough, K. P.; Blanchard, G. J. *J. Phys. Chem. B* **2006**, *110*, 6351.
(9) Lin, S.; Struve, W. S. *Photochem. Photobiol.* **1991**, *54*, 361.
(10) Mazeres, S.; Schram, V.; Tocanne, J.-F.; Lopez, A. *Biophys. J.* **1996**, *71*, 327.
(11) Mukherjee, S.; Chattopadhyay, A.; Samanta, A.; Soujanya, T. *J. Phys. Chem.* **1994**, *98*, 2809.
(12) Tsukanova, V.; Grainger, D. W.; Salesse, C. *Langmuir* **2002**, *18*, 5539.
(13) Dewitt, L.; Blanchard, G. J.; Legoff, E.; Benz, M. E.; Liao, J. H.; Kanatzidis, M. G. *J. Am. Chem. Soc.* **1993**, *115*, 12158.
(14) Garg, S. K.; NSmyth, C. P. *J. Phys. Chem.* **1965**, *69*, 1294.
(15) Nee, T. W.; Zwanzig, R. *J. Chem. Phys.* **1970**, *52*, 6353.
(16) Dong, D. C.; Winnik, M. A. *Photochem. Photobiol.* **1982**, *35*, 17.
(17) Dong, D. C.; Winnik, M. A. *Can. J. Chem.* **1984**, *62*, 2560.
(18) Kamlet, M. J.; Abboud, J. L.; Taft, R. W. *J. Am. Chem. Soc.* **1977**, *99*, 6027.
(19) Kamlet, M. J.; Hall, T. N.; Boykin, J.; Taft, R. W. *J. Org. Chem.* **1979**, *44*, 2599.
(20) Taft, R. W.; Abboud, J. L.; Kamlet, M. J. *J. Am. Chem. Soc.* **1981**, *103*, 1080.
(21) Brady, J. E.; Carr, P. W. *J. Phys. Chem.* **1982**, *86*, 3053.
(22) Reichardt, C. *Angew. Chem., Int. Ed. Engl.* **1979**, *18*, 98.
(23) Elias, H.; Dreher, M.; Neitzel, S.; Volz, H. *Z. Naturforsch., B: Anorg. Chem., Org. Chem.* **1982**, *37B*, 684.
(24) Chuang, T. J.; Eisenthal, K. B. *J. Chem. Phys.* **1972**, *57*, 5094.
(25) Johnson, C. K.; Wan, C. *Top. Fluoresc. Spectrosc.* **1997**, *5*, 43.
(26) Wan, C.; Johnson, C. K. *J. Chem. Phys.* **1994**, *101*, 10283.
(27) Wan, C.; Johnson, C. K. *Chem. Phys.* **1994**, *179*, 513.
(28) Debye, P. *Polar Molecules*; Chemical Catalog Co.: New York, 1929.
(29) Edward, J. T. *J. Chem. Educ.* **1970**, *47*, 261.
(30) Perrin, F. *J. Phys. Radium* **1936**, *7*, 1.
(31) Blanchard, G. J. Ultrafast Stimulated Emission Spectroscopy. In *Topics in Fluorescence Spectroscopy. Volume 5. Nonlinear and Two-Photon Induced Fluorescence*; Lakowicz, J. R., Ed.; Plenum Press: New York, 1997; Vol 5, p 255.
(32) Cantor, C. R.; Schimmel, P. R. *Biophysical Chemistry*; Mir: Moscow, 1984; Vol 1.
(33) Dutt, G. B.; Srivatsavoy, V. J. P.; Sapre, A. V. *J. Chem. Phys.* **1999**, *110*, 9623.
(34) Blanchard, G. J. *J. Phys. Chem.* **1988**, *92*, 6303.
(35) Blanchard, G. J.; Cihal, C. A. *J. Phys. Chem.* **1988**, *92*, 5950.
(36) Stevenson, S. A.; Blanchard, G. J. *J. Phys. Chem.* A **2006**, *110*, 3426.
(37) Srinivas, G.; Bhattacharyya, S.; Bagchi, B. *J. Chem. Phys.* **1999**, *110*, 4477.
(38) Kivelson, D.; Spears, K. G. *J. Phys. Chem.* **1985**, *89*, 1999.
(39) Madden, P.; Kivelson, D. *J. Phys. Chem.* **1982**, *86*, 4244.
(40) Dote, J. L.; Kivelson, D. *J. Phys. Chem.* **1983**, *87*, 3889.
(41) Dote, J. L.; Kivelson, D.; Knobler, C. M. *J. Chem. Phys.* **1980**, *73*, 3519.
(42) Dote, J. L.; Kivelson, D.; Schwartz, R. N. *J. Phys. Chem.* **1981**, *85*, 2169.
(43) Cross, A. J.; Simon, J. D. *J. Chem. Phys.* **1987**, *86*, 7079.
(44) Hubbard, J. B.; Wolynes, P. G. *J. Chem. Phys.* **1978**, *69*, 998.
(45) van der Zwan, G.; Hynes, J. T. *J. Phys. Chem.* **1985**, *89*, 4181.
(46) Vijayadamodar, G. V.; Chandra, A.; Bagchi, B. *Chem. Phys. Lett.* **1989**, *161*, 413.
(47) Simon, J. D.; Thompson, P. A. *J. Chem. Phys.* **1990**, *92*, 2891.
(48) Blanchard, G. J.; Wirth, M. J. *J. Phys. Chem.* **1986**, *90*, 2521.
(49) Dutt, G. B.; Raman, S. *J. Chem. Phys.* **2001**, *114*, 6702.
(50) Horng, M.-L.; Gardecki, J. A.; Maroncelli, M. *J. Phys. Chem. A* **1997**, *101*, 1030.
(51) Jiang, Y.; McCarthy, P. K.; Blanchard, G. J. *Chem. Phys.* **1994**, *183*, 249.
(52) Dutt, G. B. *ChemPhysChem* **2005**, *6*, 413.
(53) Maroncelli, M.; MacInnis, J.; Fleming, G. R. *Science* **1989**, *243*, 1674.